THE JOURNAL OF BIOLOGICAL CHEMISTRY
Vol. 278, No. 39, Issue of September 26, pp. 37015–37023, 2003

Printed in U.S.A.

Structural and Functional Adaptations to Extreme Temperatures in Psychrophilic, Mesophilic, and Thermophilic DNA Ligases*

Received for publication, May 16, 2003
Published, JBC Papers in Press, July 10, 2003, DOI 10.1074/jbc.M305142200

Daphné Georlette‡, Benjamin Damien§, Vinciane Blaise‡, Eric Depiereux§, Vladimir N. Uversky¶‖, Charles Gerday‡, and Georges Feller‡**

From the ‡Laboratory of Biochemistry, Institute of Chemistry B6, University of Liège, B-4000 Liège, Belgium, the §Unité de Biologie Moléculaire, Département de Biologie, Facultés Universitaires Notre-Dame de la Paix, B-5000 Namur, Belgium, the ¶Institute for Biological Instrumentation, Russian Academy of Sciences, Pushchino, Moscow Region 142290, Russia, and the ‖Department of Chemistry and Biochemistry, University of California, Santa Cruz, California 95064

Psychrophiles, host of permanently cold habitats, display metabolic fluxes comparable to those exhibited by mesophilic organisms at moderate temperatures. These organisms have evolved by producing, among other peculiarities, cold-active enzymes that have the properties to cope with the reduction of chemical reaction rates induced by low temperatures. The emerging picture suggests that these enzymes display a high catalytic efficiency at low temperatures through an improved flexibility of the structural components involved in the catalytic cycle, whereas other protein regions, if not implicated in catalysis, may be even more rigid than their mesophilic counterparts. In return, the increased flexibility leads to a decreased stability of psychrophilic enzymes. In order to gain further advances in the analysis of the activity/flexibility/stability concept, psychrophilic, mesophilic, and thermophilic DNA ligases have been compared by three-dimensional-modeling studies, as well as regards their activity, surface hydrophobicity, structural permeability, conformational stabilities, and irreversible thermal unfolding. These data show that the cold-adapted DNA ligase is characterized by an increased activity at low and moderate temperatures, an overall destabilization of the molecular edifice, especially at the active site, and a high conformational flexibility. The opposite trend is observed in the mesophilic and thermophilic counterparts, the latter being characterized by a reduced low temperature activity, high stability and reduced flexibility. These results strongly suggest a complex relationship between activity, flexibility and stability. In addition, they also indicate that in cold-adapted enzymes, the driving force for denaturation is a large entropy change.

The temperature range in which biological activity has been detected extends from −20 °C, the temperature recorded in the brine veins of Arctic or Antarctic sea ice (1), to 113 °C, the temperature at which the archae *Pyrolobus fumarii* is still able to grow (2). Although numerous investigations have been carried out on thermophilic microorganisms and on their molecular components, especially enzymes, the efforts devoted to cold-adapted microorganisms have been comparatively limited despite their tremendous biotechnological (1, 3–5) and fundamental (1, 6–8) applications. Indeed, the biochemical and physiological bases of cold adaptation, which include, for example, regulation of gene expression by low temperatures, membrane adaptation in relation with the homeoviscosity concept, and the activity/stability relationships sustaining the catalytic efficiency of cold-adapted enzymes, are still poorly understood.

In permanent cold habitats, low temperatures have constrained psychrophiles to develop among other peculiarities enzymatic tools allowing metabolic rates compatible to life that are close to those of temperate organisms. Thermal compensation in these enzymes is reached, in most cases, through a high catalytic efficiency at low and moderate temperatures (for review, see Ref. 9 and 10). The emerging picture is that this increased catalytic efficiency is attributed to an increase of the plasticity or flexibility of appropriate parts of the molecular structure in order to compensate for the lower thermal energy provided by the low temperature habitat. This plasticity would enable a good complementarity with the substrate at a low energy cost, thus explaining the high specific activity of psychrophilic enzymes. In return, this flexibility would be responsible for the weak thermal stability of cold-adapted enzymes. This relationship between activity, flexibility and stability constitutes a hot topic and represents a central issue in the adaptation of proteins to various environments. Moreover, it is believed that all proteins evolve through a balanced compromise between these features, *i.e.* structural rigidity allowing the retention of a specific three-dimensional-conformation at the physiological temperature and in contrast flexibility, allowing the protein to perform its catalytic function. In the context of temperature adaptation of enzymes, it is assumed that high temperatures require stable protein structure and activity, whereas high enzyme activity is mandatory at low temperatures.

While the common trait of a low conformational stability in cold-adapted enzymes has been demonstrated (see Ref. 11 for review), the stability/flexibility relationship is still controversial since some authors consider that the instability of psychrophilic enzymes is due to a random genetic drift (12). Moreover, if the decreased stability of cold-adapted enzymes is well documented, there is however, no direct experimental evidence of an increased flexibility. Besides, controversial results were obtained when the flexibility of a few psychrophilic enzymes was investigated by measuring hydrogen-deuterieum exchange rates. In the case of 3-isopropylmalate dehydrogenase (13), while the psychrophilic and mesophilic enzymes were found

* This work was supported by the European Union (Grant CT970131), the Région Wallonne (Grants Bioval 981/3860, Bioval 981/3848, Initiative 114705), the FNRS Belgium (Grant 2.4515.00), and the Institut Polaire Français. The costs of publication of this article were defrayed in part by the payment of page charges. This article must therefore be hereby marked "*advertisement*" in accordance with 18 U.S.C. Section 1734 solely to indicate this fact.

** To whom correspondence should be addressed: Laboratory of Biochemistry, Institute of Chemistry B6, University of Liège, B-4000 Liège, Belgium. Tel.: 32-4-366-33-43; Fax: 32-4-366-33-64; E-mail: gfeller@ulg.ac.be.

more flexible than the thermophilic counterpart, the psychrophile was however more rigid than the mesophile. Nevertheless, in this case, the technique suffered from the disadvantage of being a measure of the accessibility of deeply buried residues, and thus did not detect local flexibility, in particular that associated with the active site which is generally quite accessible. Using a similar technique, Fields (14) showed that while a psychrophilic and a mesophilic lactate dehydrogenases had similar flexibility at 2 °C, the global flexibility of the psychrophile was significantly larger at 23 °C. In addition to the lack of data about the flexibility of cold-adapted enzymes, information on the thermodynamics of inactivation and unfolding is also missing and the few available reports are controversial. Indeed, Siddiqui *et al.* (15) proposed that the thermolability of psychrophilic enzymes is due to enthalpic effects, while others (16–18) found this to be entropically driven. Further studies are thus required to resolve whether an unfavorable entropic or enthalpic contribution determines the irreversible unfolding and inactivation of these enzymes.

In attempt to elucidate how stability, catalytic activity, and conformational flexibility are connected in psychrophilic enzymes, we have investigated three structurally homologous NAD^+-dependent DNA ligases. The psychrophilic DNA ligase from the Antarctic bacterium *Pseudoalteromonas haloplanktis* (*Ph*lig)[1] has been overexpressed and characterized (19), highlighting an increased catalytic efficiency as well as an increased thermolability of the enzyme. Cold adaptation of *Ph*lig is believed to be due to a decreased level of arginine and proline residues, as well as an overall destabilization of its N-terminal domain (19). The mesophilic reference chosen is the DNA ligase form *Escherichia coli* (*Ec*lig) (20) and the thermophilic homologue is the *Thermus scotoductus* DNA ligase (*Ts*lig) (21). The three enzymes are of a similar size, share all the properties common to NAD^+-dependent DNA ligases, but are adapted to different extremes of the temperature scale (19), therefore constituting an adequate series of homologous enzymes for temperature adaptation studies. In the present work, the overall destabilization of *Ph*lig is examined with the help of three-dimensional modeling and investigation of solvent-exposed hydrophobic clusters. In addition, the intricate relationship between activity, flexibility and stability in *Ph*lig is analyzed by comparison of its temperature dependent activity, conformational flexibility, and thermal and chemical stabilities with its mesophilic and thermophilic counterpart *Ec*lig and *Ts*lig, respectively.

EXPERIMENTAL PROCEDURES

Three-dimensional Modeling—The target sequences for modeling are the NAD^+-dependent DNA ligases from *P. haloplanktis*, *E. coli*, and *T. scotoductus*. The best template for the three proteins was 1DGS.A, the homologue NAD^+-DNA ligase of *T. filiformis* (22). The modeling, minimizations and molecular dynamics procedures were described elsewhere.[2] The equilibrium temperatures chosen, known as the optimal organism temperature, were 277, 310, and 354 K, for *P. haloplanktis*, *E. coli*, and *T. scotoductus*, respectively.

Protein Preparation and Assays—The recombinant cold-adapted NAD^+-dependent DNA ligase (*Ph*lig) was overexpressed at 18 °C in *E. coli* BL21(DE3) as previously described (19), except that the growth was performed in TB medium (12 g/liter tryptone, 24 g/liter yeast extract, 4 ml/liter glycerol, 12.54 g/liter K_2HPO_4, 2.32 g/liter KH_2PO_4, pH 7) containing 50 μg ml^{-1} kanamycin, and that induction was performed when OD_{600} reached ~4. The cold His-tagged enzyme was then purified by Ni^{2+}-Hitrap Chelating followed by thrombin digestion, second Ni^{2+}-Hitrap Chelating to separate untagged protein from the undigested ligase, and Mono Q HR 5/5, as described previously (19). Plasmid encoding *E. coli* DNA ligase was a generous gift from V. Sriskanda and S. Shuman (20). The pET-*Eco*LIG plasmid (20) was digested with *Nde*I and *Bam*HI and the insert cloned into pET23a plasmid, leading to the overexpression of an untagged protein. The recombinant *Ec*lig was overexpressed at 37 °C in *E. coli* BL21(DE3) as previously described (20), except that the growth was performed in TB-ampicillin medium containing 100 μg ml^{-1} ampicillin, and that induction was performed when OD_{600} reached ~3. The mesophilic protein was purified according to a protocol established for *T. scotoductus* DNA ligase (*Ts*lig) (23), except that the heatings treatments were replaced by a DEAE-agarose column chromatography. Plasmid encoding *Ts*lig was a kind gift from Z. O. Jónsson and G. Eggertsson (Reykjavik, Iceland) (21). The recombinant wild-type *Ts*lig was overexpressed and purified by two successive heatings (65 and 80 °C), followed by Hi-Trap Heparin and Mono Q HR chromatographic steps, as described (23). Protein concentration was determined with the Coomassie Protein Assay Reagent (Pierce), using bovine serum albumin as standard. The final yield was ~100 mg, ~250 mg, and ~55 mg per liter of culture for *Ph*lig, *Ec*lig, and *Ts*lig respectively. N-terminal sequencing confirmed the integrity of recombinant proteins. Enzyme activity was determined using a fluorimetric assay, as described previously (19).

Adenylation Assays—In order to compare DNA ligases in a similar adenylation state, enzyme stock solutions were adenylated by adding an excess of β-NAD^+ (24). The ratio $[NAD^+]$/[DNA ligase] was ~80. The adenylated mixtures were then incubated at 10 °C (*Ph*lig), 25 °C (*Ec*lig), and 65 °C (*Ts*lig) for 30 min and then cooled rapidly on ice. Protein solutions were dialyzed against appropriate buffer before experiments.

Fluorescence Measurements—Both intrinsic and ANS fluorescence measurements were recorded on an Aminco SLM 8100 spectrofluorimeter. Thermal denaturation (scan rate 1 °C/min) of the DNA ligases was monitored by recording the fluorescence intensity change at 330 nm, using a protein concentration of 50 μg/ml (0.66 μM) in 20 mM phosphate sodium, 50 mM NaCl, pH 7.6, with excitation at 280 nm (2-nm band pass) and emission at 330 nm (4-nm band pass). Data were normalized using the pre- and post-transition baseline slopes as described (25) and were fit according to a three-state model (26).

ANS fluorescence measurements were performed at 25 °C except for *Ph*lig (15 °C), using a protein concentration of 25 μg/ml (0.33 μM) in 20 mM phosphate sodium, 50 mM NaCl, pH 7.6, with excitation at 390 nm (2-nm band pass), and emission (4-nm band pass) spectra recorded from 420 to 600 nm (scan speed 350 nm min^{-1}). The fluorescence spectra were corrected for the background fluorescence of ANS. The ratio [ANS]/[ligase] was ~200 using $\epsilon_{350\ nm}$ = 4950 M^{-1} cm^{-1} for ANS. Thermal unfolding of samples containing ANS was performed at a scan rate of 1 °C/min. In this case, the recorded fluorescence spectra were corrected for the background fluorescence of ANS at the corresponding temperature.

Dynamic Quenching of Fluorescence—The conformational resiliences of *Ph*lig, *Ec*lig, and *Ts*lig were characterized by acrylamide-induced fluorescence quenching. Samples were prepared in 20 mM sodium phosphate buffer, 50 mM NaCl, pH 7.6, and the protein concentrations (~50 μg/ml) were adjusted to provide an optical density at the excitation wavelength less than 0.1. Aliquots of a 1.2 M acrylamide stock solution were consecutively added to 1 ml protein solution in order to increase acrylamide concentration by ~5 mM steps. Experiments were performed on an Aminco SLM 8100 spectrofluorimeter at 10 and 25 °C, using excitation at 280 nm with fluorescence emission set at 330 nm (excitation and emission slit widths were 1 and 4, respectively) and the fluorescence intensities were recorded for 30 s. Data, that are the mean of three experiments, were corrected for the dilution effects and for the absorptive screening caused by acrylamide ($\epsilon_{280\ nm}$ = 4.3 M^{-1} cm^{-1} for acrylamide). Quenching data were plotted as the ratio of fluorescence in the absence of quencher (F_0) to the intensity in the presence of quencher (F) against quencher concentration. The resulting data were fit to dynamic parameters according to the Stern-Volmer relation shown in Equation 1,

$$F_0/F = 1 + K_{SV}[Q] \quad \text{(Eq. 1)}$$

where K_{SV} is the Stern-Volmer quenching constant and [Q] the quencher concentration (27).

Differential Scanning Calorimetry (DSC)—Measurements were performed using a MicroCal MCS-DSC instrument as detailed (28). Samples were dialyzed overnight against 30 mM MOPS, 50 mM KCl, pH 7.6. In order to decrease aggregation, a non-detergent sulfobetaine (3-(1-

[1] The abbreviations used are: *Ph*lig; *P. haloplanktis* DNA ligase; FI, fluorescence intensity; DSC, differential scanning calorimetry; *Ec*lig, *E. coli* DNA ligase; *Ts*lig, *T. scotoductus* DNA ligase; ANS, 8-anilino-1-naphthalene sulfonic acid; MOPS, 4-morpholinepropanesulfonic acid.

[2] D. Georlette, V. Blaise, F. Bouillenne, B. Damien, S. H. Thorbjarnardottir, E. Depiereux, C. Gerday, V. N. Uversky, and G. Feller, submitted manuscript.

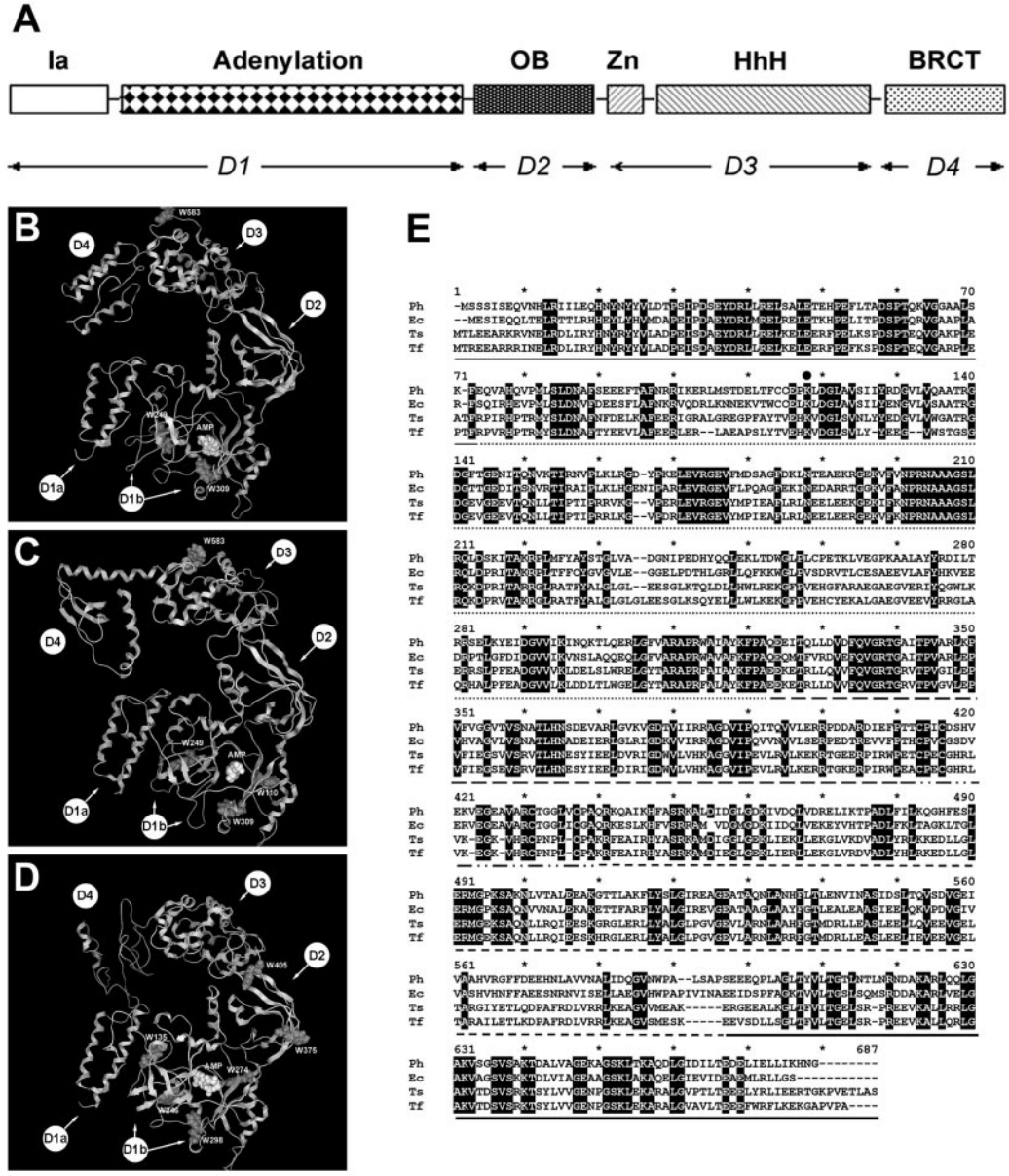

FIG. 1. **Domain structure of *Ph, Ec, and Ts* DNA ligases.** *A*, NAD^+-dependent DNA ligases are depicted as a linear assortment of conserved structural domains (*Ia*, adenylation, *OB* (oligomer-binding) fold, Zn-binding, *HhH* (helix-hairpin-helix), and BRCT (BRCA1 C-terminus) in four domains D1–D4. *B–D*, schematic view of the three-dimensional structure of *Ph*lig (*B*), *Ec*lig (*C*), and *Ts*lig (*D*). Tryptophan (W) residues are located as *gray filled structures*. *Ph*lig, *Ec*lig, and *Ts*lig contain 3, 4, and 6 W, respectively. The covalently bound AMP moiety is located as a *white filled structure*. *E*, multiple sequence alignment (ClustalW) of NAD^+-dependent DNA ligases. Every 10^{th} residue is marked with an *asterisk* symbol. Conserved residues in the four DNA ligases are *boxed* in *black*. The *solid circle symbol* (●) indicates the AMP-binding lysine (K) residue of bacterial DNA ligases. Domain Ia is shown with a *thin continuous line*; Adenylation domain is shown with a *dotted line* (. . .); OB-fold domain is shown with *long dashed line* (—); Zn-binding domain is shown with a "*dash-dot-dot*" *line*; HhH domain is shown with a *short dashed line* (– –), and BRCT domain is shown with a *thick continuous line*. *Ph*, *P. haloplanktis* DNA ligase; *Ec*, *E. coli* DNA ligase; *Ts*, *T. scotoductus* DNA ligase; *Tf*, *T. filiformis* DNA ligase.

pyridinio)-1-propane sulfonate) was added prior to DSC experiment (29), to a final concentration of 0.5 M for *Ph*lig and *Ec*lig, and 0.75 M for *Ts*lig. Protein concentration was determined with the Coomassie Protein Assay Reagent (Pierce), and was ~4 mg/ml except for *Ph*lig (~7 mg/ml). Thermograms were analyzed according to a non-two-state model in which T_m, ΔH_{cal}, and ΔH_{eff} of individual transitions are fitted independently using the MicroCal Origin software (version 2.9). The magnitude and source of the errors in the T_m and enthalpies values have been discussed elsewhere (30). Fitting standard errors on a series of three DSC measurements made under the same conditions in the present study were found to be ± 0.1 K on T_m and ±4% on both enthalpies. All scans were found to be irreversible under the experimental conditions used for these studies. Kinetically driven unfolding was recorded at two different scan rates (0.4 and 1 K min^{-1} for *Ph*lig, and 1 and 2 K min^{-1} for *Ec*lig), and the rate constant k_{denat} was calculated from the relation shown in Equation 2 (31),

$$k = vC_p/(\Delta H_{cal} - Q) \quad \text{(Eq. 2)}$$

where v represents the scan rate (K min^{-1}), C_p the excess heat capacity at a given temperature, ΔH_{cal} the total heat of the process, and Q the heat evolved at the given temperature.

GdmCl-induced Unfolding—Approximately 25 μg/ml ($A_{280\ nm} < 0.1$) protein samples in 50 mM phosphate sodium, 50 mM NaCl, pH 7.6, were incubated overnight at 25 °C (18 °C for the cold-adapted *Ph*lig), in defined guanidine hydrochoride (GdmCl) concentrations, and unfolding was monitored by intrinsic fluorescence analysis. The pH was checked to ensure a constant value throughout the whole transition, and the denaturant concentration was determined from refractive index measurements (25) using a R5000 hand refractometer from Atago. Relative fluorescence was measured on an Aminco SLM 8100 spectrofluorimeter at 25 °C, except for *Ph*lig (18 °C), at an excitation wavelength of 280 nm (2-nm band pass) and at an emission wavelength of 330 nm (4-nm band

TABLE I
Composition and surface accessibility of the active site (adenylation domain) of Phlig, Eclig, and Tslig

	*Ph*lig	*Ec*lig	*Ts*lig
Composition			
Number of amino acids (aa) forming the active site	248	248	246
Number of positively charged aa (basic)	37 (15%)	36 (14%)	42 (17%)
Number of negatively charged aa (acidic)	35 (14%)	33 (13%)	39 (15%)
Number of neutral aa	52 (21%)	45 (18%)	36 (14%)
Number of nonpolar aa	124 (50%)	134 (54%)	129 (52%)
Surface accessibility (Å^2)			
Recalculated accessible surface	14375	13575	13888
Surface of positively charged aa (basic)	4339 (30%)	4329 (31%)	5629 (40%)
Surface of negatively charged aa (acidic)	2579 (18%)	2510 (18%)	3220 (23%)
Surface of neutral aa	2911 (20%)	2519 (18%)	1312 (9%)
Surface of nonpolar aa	4546 (32%)	4217 (31%)	3727 (26%)

TABLE II
Composition of the accessible surface of Phlig, Eclig, and Tslig

	*Ph*lig	*Ec*lig	*Ts*lig
Surface accessibility (Å^2)			
Recalculated accessible surface	36183	36085	36626
Neutral accessible surface	3254 (9%)	2362 (7%)	2269 (6%)
Hydrophobic accessible surface	7994 (22%)	6468 (18%)	6270 (17%)
Hydrophilic accessible surface	24935 (69%)	27255 (75%)	28087 (77%)
positively charged	9202 (25%)	11800 (33%)	13129 (36%)
negatively charged	7184 (20%)	9187 (25%)	8834 (24%)

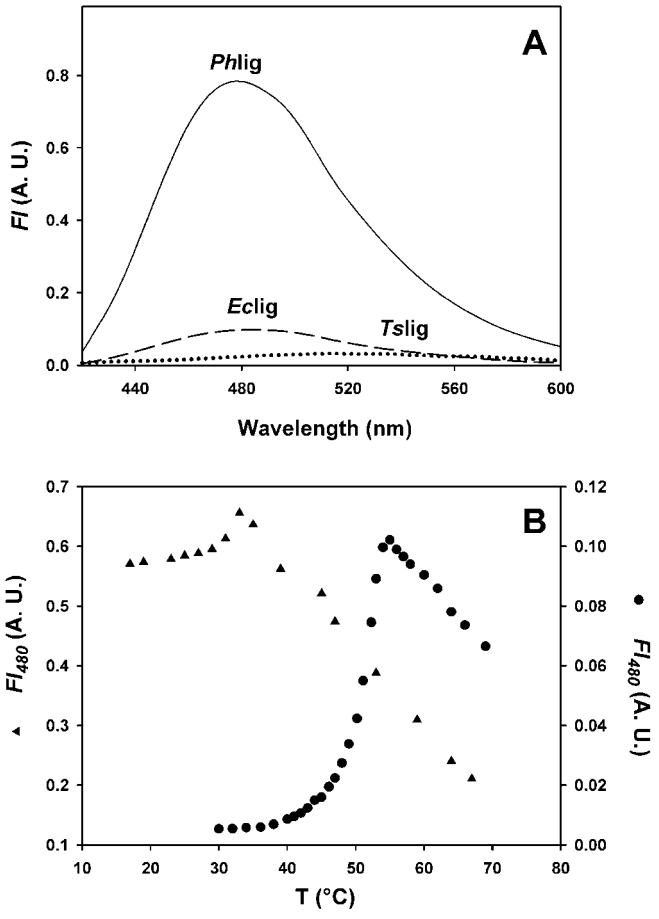

FIG. 2. **ANS fluorescence intensity.** *A*, ANS fluorescence spectra of *Ph*lig, *Ec*lig, and *Ts*lig in the native state. *B*, temperature dependence of ANS binding by *Ph*lig (▲) and *Ec*lig (●), measured by the intensity of ANS fluorescence at 480 nm (λ_{ex} 390 nm).

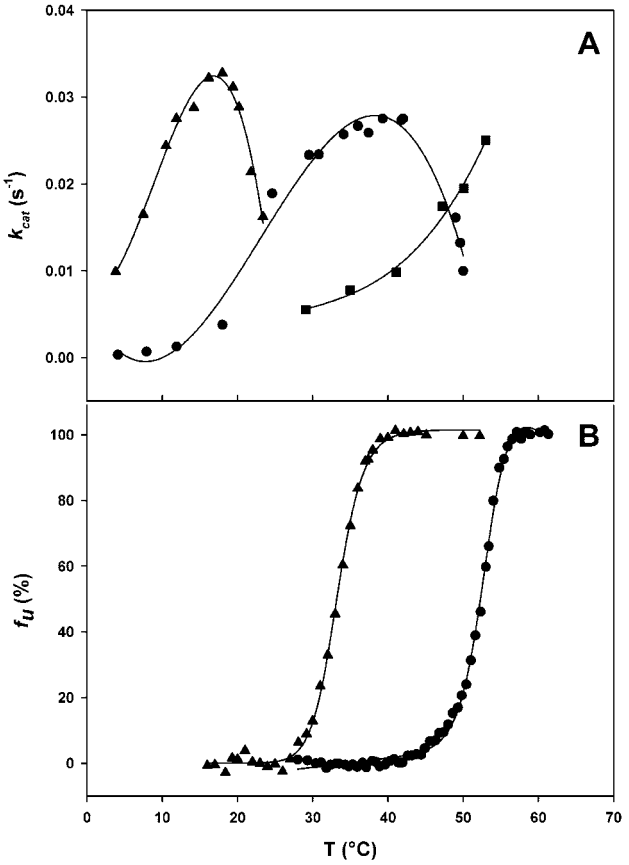

FIG. 3. **Thermodependence of activity (*A*) and denaturation as recorded by fluorescence emission (*B*).** Compared with *Ec*lig (●) and *Ts*lig (■), the cold-adapted *Ph*lig (▲) is characterized by: (i) a shift of the optimal activity toward low temperatures, (ii) an increased specific activity at low and moderate temperatures, and (iii) a low stability of its active site.

pass), except *Ts*lig (λ_{em} 333 nm). Unfolding of the three DNA ligases *Ph*lig, *Ec*lig, and *Ts*lig was fully reversible since they regained native conformation following renaturation after complete denaturation in 7 M GdmCl. Fluorescence spectroscopy data were normalized using the pre- and post-transition baseline slopes as described (25). The transition curves obtained were analyzed using a three-state model (N↔I↔U) (26).

Determination of Activation Parameters—Thermodynamic parameters of activation were calculated as described (32), using Equations 3–5,

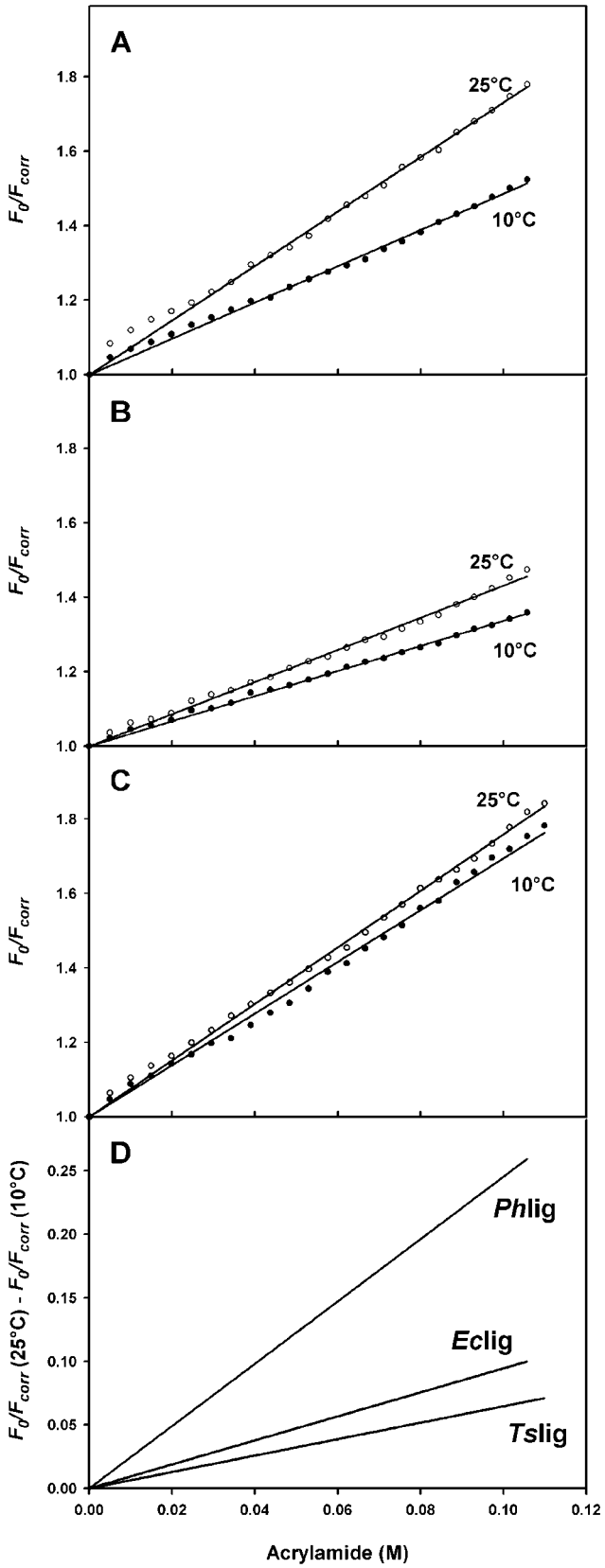

FIG. 4. **Stern-Volmer plots of fluorescence quenching by acrylamide.** Fluorescence quenching at 10 °C (●) and 25 °C (○) of *Ph*lig (*A*), *Ec*lig (*B*) and *Ts*lig (*C*). S.D. was within 2% of the experimental values. The variation of fluorescence quenching between 10 and 25 °C is obtained by subtracting the regression lines of Stern-Volmer plots at individual temperatures (*D*). According to Equation 1, the quenching constant K_{sv} corresponding to the plot slope are 4.87(±0.07), 3.37(±0.04), and 6.95(±0.10) M^{-1} at 10 °C and 7.32(±0.12), 4.32(±0.06), and 7.59(±0.08) M^{-1} at 25 °C for *Ph*lig, *Ec*lig, and *Ts*lig, respectively.

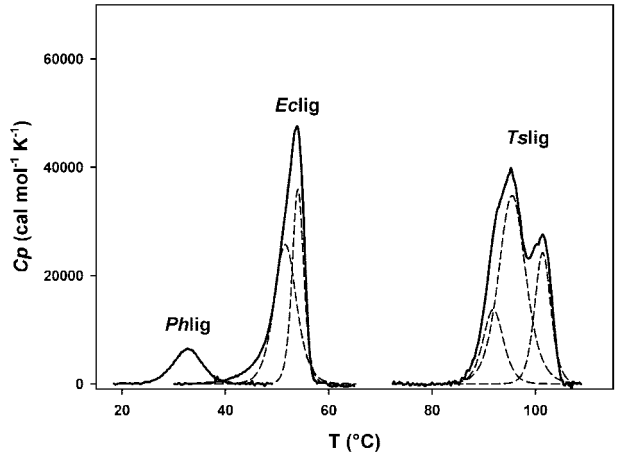

FIG. 5. **Thermal unfolding of DNA ligases recorded by DSC.** *Ph*lig is characterized by a lower T_{max} (*top of the transition*) and ΔH_{cal} (*area under the transition*) than *Ec*lig and *Ts*lig. In addition, *Ph*lig displays one calorimetric domain, whereas *Ec*lig and *Ts*lig are characterized by two and three calorimetric domains, respectively (deconvolutions are in *short dashed lines*). All thermograms are baseline subtracted and normalized for protein concentrations.

$$\Delta G^{\#} = RT \times \left(\ln\frac{k_B T}{h} - \ln k\right) \quad \text{(Eq. 3)}$$

$$\Delta H^{\#} = E_a - RT \quad \text{(Eq. 4)}$$

$$\Delta S^{\#} = (\Delta H^{\#} - \Delta G^{\#})/T \quad \text{(Eq. 5)}$$

where k_B is the Boltzmann constant (1.3805 10^{-23} J K^{-1}), h the Planck constant (6.6256 10^{-34} J s), k (s^{-1}) the rate constant at temperature T (K), E_a the activation energy of the reaction, and R (8.314 J mol^{-1} K^{-1}) the gas constant.

RESULTS

Molecular Model of Adenylated Phlig, Eclig, and Tslig—The amino acid sequences of *Ph*lig, *Ec*lig, and *Ts*lig show 45, 45, and 87% identity with *T. filiformis* (*Tf*lig) DNA ligase, allowing us to build three-dimensional models from the known x-ray structure (Fig. 1, *B–D*). The final models of *Ph*lig, *Ec*lig, and *Ts*lig can be superimposed, showing a strong conservation of the active site architecture, of the main secondary structures, and of the overall fold. These monomeric enzymes are folded into four discrete domains characterizing NAD^+-dependent DNA ligases (22) (Fig. 1, *A* and *E*), *i.e.* Domain 1 (containing Ia and adenylation subdomains), Domain 2 (OB-fold domain), Domain 3 (Zn-finger and HhH subdomains), and Domain 4 (BRCT or BRCA C-terminal-related domain). As shown for *Tf* DNA ligase (22), the circular arrangement of the four domains leads to a hole sufficiently large to hold a double-stranded DNA.

Sequence alignment reveals that the psychrophilic DNA ligase contains all the conserved boxes that have previously been described in eubacterial DNA ligases (Fig. 1*E*). Moreover, the recent determination of the structure of *Tf*lig (22), as well as the investigation of Domain Ia of *Ec*lig (33) have pointed out essential residues implicated in catalysis, that appear to be conserved among NAD^+-dependent DNA ligases adapted to different temperatures. To further characterize the active site of the psychrophilic enzyme, the number as well as the surface of positively charged, negatively charged, neutral, and nonpolar amino acids of the adenylation domain were determined (Table I). The main trend is a decrease in the number and mainly in the accessible surface of neutral side chains form *Ph*lig to *Ec*lig and *Ts*lig. This is accompanied by a decrease of the accessible surface of nonpolar side chains and an increase of the accessible charged surfaces. As a result, the active site of the psychrophilic ligase is characterized by an excess of hydro-

TABLE III
Thermodynamic parameters of heat-induced unfolding of Phlig, Eclig and Tslig

Enzyme	T_{max}[a]	Transitions	T_m[c]	ΔH_{cal}	$\Sigma \Delta H_{cal}$
	°C	n[b]	°C	*kJ mol*$^{-1}$	*kJ mol*$^{-1}$
*Ph*lig	32.7	1	32.7	193	193
*Ec*lig	53.9	2	51.6	615	1059
			54.1	444	
*Ts*lig	95.2	3	91.8	301	1729
	101.3		95.6	1009	
			101.4	419	

[a] T_{max} corresponds to the temperature at the top of the peak.
[b] n refers to the number of calorimetric domains identified by deconvolution of DSC thermograms.
[c] T_m is the melting point of the unfolding transition.

phobic surfaces and reduced charged surfaces when compared with the adenylation domain of the thermophilic enzyme. A similar trend is observed when the whole molecule is analyzed (Table II). As shown in Table II, the psychrophilic enzyme displays an increased exposure of hydrophobic residues to the solvent, whereas the thermophilic DNA ligase shows an increased hydrophilic accessible surface area, including an increase of the charged accessible surface. Such discrepancies probably lead to improved electrostatic interactions in the thermophilic ligase that are likely to stabilize the enzyme at high temperatures, whereas the excess of hydrophobic surfaces in *Ph*lig represents an entropy-driven destabilizing factor.

ANS Fluorescence—It is well known that the interaction of hydrophobic fluorescent probes such as 8-anilino-1-naphtalenesulfonic acid (ANS) with the exposed hydrophobic sites on the surface of native protein results in a considerable increase of the dye fluorescence intensity and a blue shift of its fluorescence spectrum (34, 35). As the three-dimensional modeling predicted an increased exposure of hydrophobic residues to the solvent in *Ph*lig, the binding of ANS was investigated in the three adenylated DNA ligases.

As seen in Fig. 2*A*, no significant binding of ANS can be observed with the native adenylated *Ts*lig. In the case of *Ec*lig, a slight binding is detected, suggesting the exposure of some hydrophobic patches at the surface of the native enzyme. By contrast, strong enhancement of ANS fluorescence is recorded for *Ph*lig, underlining a significant population of solvent-accessible nonpolar clusters in the native enzyme. Changes in ANS fluorescence were also monitored during thermal denaturation. In the case of *Ph*lig (Fig. 2*B*), a slight increase of ANS binding is observed when increasing the temperature, which reaches a maximum around 33 °C (corresponding to a maximal surface exposition of hydrophobic clusters), and then decreases to an intensity lower than that of the native enzyme. *Ec*lig displays a similar behavior (Fig. 2*B*), except that the increase in ANS fluorescence is more pronounced when increasing the temperature, reaches a maximum around 55 °C and then decreases at higher temperatures, but still exhibits significant ANS fluorescence, at a level significantly higher than that of the native enzyme. Such result suggests that *Ec*lig is more prone to form aggregates at high temperatures. Such aggregates are still able to bind ANS, leading to the observed ANS signal at high temperatures. The high stability of *Ts*lig (see below) did not allow monitoring ANS changes occurring upon thermal denaturation.

Thermodependence of Activity—The thermodependence of activity of *Ph*lig, *Ec*lig, and *Ts*lig is shown in Fig. 3*A*. It can be seen that the maximal activity of *Ph*lig (16 °C) is shifted toward low temperatures (42 °C for *Ec*lig), reflecting its weak stability. Denaturation of the DNA substrate at high temperatures did not allow the determination of the optimal temperature for *Ts*lig activity, but our results indicate that this value is higher

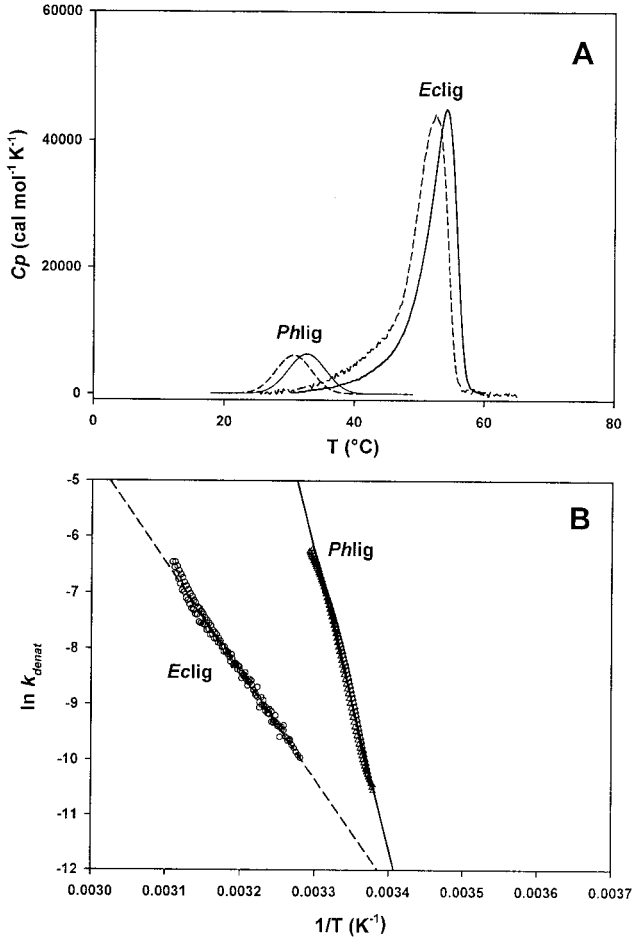

FIG. 6. **Irreversible thermal unfolding as monitored by DSC.** *A*, DSC profiles recorded at scan rates of 0.4 and 1 K min^{-1} for the cold-adapted *Ph*lig and 1 and 2 K min^{-1} for the mesophilic *Ec*lig. *B*, Arrhenius plots for the irreversible denaturation of *Ph*lig (*triangles*, *continuous line*) and *Ec*lig (*circles*, *short dashed line*). For both enzymes, symbols include experiments performed at the two different scan rates.

than 55 °C. This highlights a clear link between optimal activity acquisition and thermal adaptation. It should be noted in Fig. 3*A* that *Ph*lig exhibits significantly higher reaction rates (k_{cat}) at low and moderate temperatures as compared with *Ec*lig and *Ts*lig. Comparison of the temperature dependence of activity (Fig. 3*A*) and thermal unfolding recorded by fluorescence emission (Fig. 3*B*) also reveals an interesting behavior of *Ph*lig. Indeed, the maximal activity of *Ec*lig closely corresponds to the beginning of the unfolding transition, therefore explaining the loss of activity at higher temperatures. By contrast, the maximal activity of *Ph*lig is reached 10 °C before unfolding and the enzyme is inactivated at the beginning of the transition. This suggests an extremely labile active site or catalytic intermediates in the cold-adapted enzyme.

Fluorescence Quenching—The conformational flexibility of the three DNA ligases was probed by dynamic fluorescence quenching, using acrylamide as quencher. Fig. 4 shows the Stern-Volmer plots for *Ph*lig (Fig. 4*A*), *Ec*lig (Fig. 4*B*), and *Ts*lig (Fig. 4*C*) at 10 and 25 °C and clearly demonstrates a higher accessibility of tryptophan (W) residues in *Ph*lig as the temperature increases. Absolute values of the Stern-Volmer quenching constant (K_{sv}) can be compared only if the number and location of W residues in the structures are identical, as well as their environment. This condition is not met for the three related DNA ligases and thus, the variation of the K_{sv} with temperature becomes the relevant parameter. Indeed, as shown in Fig. 1*B*, *Ph*lig contains 3 tryptophan residues; Trp-

TABLE IV
Thermodynamic parameters for the irreversible unfolding

		E_a	$\Delta G^{\#}$	$\Delta H^{\#}$	$T\Delta S^{\#}$
		kJ mol^{-1}	*kJ mol*$^{-1}$	*kJ mol*$^{-1}$	*kJ mol*$^{-1}$
For k_{denat} = 3.4 10^{-5} s^{-1}	T				
*Ph*lig	300.2°K	424.7	93.5	422.2	328.7
*Ec*lig	314.5°K	164.7	98.1	162.1	64.0
For T = 308.2°K	k_{denat}				
*Ph*lig	2.7 10^{-2} s^{-1}	424.7	84.8	422.1	337.3
*Ec*lig	9.3 10^{-5} s^{-1}	164.7	99.4	162.1	62.7

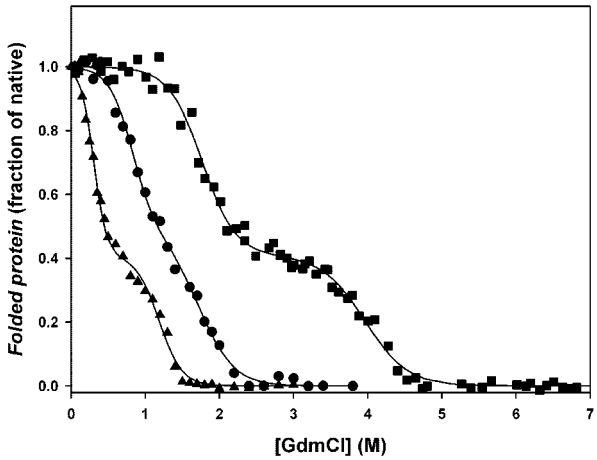

FIG. 7. **Equilibrium unfolding of *Ph*lig (▲), *Ec*lig (●), and *Ts*lig (■) as recorded by fluorescence emission.** Data were analyzed according to a three-state reaction. The *solid lines* represent the best fits of the data analyzed according to a three-state reaction.

249 is rather buried, whereas Trp-309 and Trp-583 are relatively and fully accessible to the solvent, respectively. *Ec*lig contains an additional tryptophan, Trp-110. This tryptophan is totally buried, whereas Trp-309 is rather buried and Trp-249 and Trp-583 are relatively accessible to the solvent (Fig. 1*C*). Finally, *Ts*lig contains 6 tryptophan residues; Trp-135, Trp-246, Trp-274, and Trp-405 are rather buried, whereas Trp-298 and Trp-375 are relatively accessible to the solvent (Fig. 1*D*). Fig. 4*D* illustrates the difference curves (25 °C − 10 °C) for the Stern-Volmer plots. The higher slope observed for *Ph*lig is indicative of a greater effect of temperature on the acrylamide quenching of the protein fluorescence. This indicates a greater permeability of this enzyme to acrylamide in a temperature range where the native state prevails.

Thermal Stability of DNA Ligases—Thermal unfolding of *Ph*lig, *Ec*lig, and *Ts*lig was monitored by differential scanning calorimetry (DSC). A non-detergent sulfobetaine was added prior to DSC experiments (see "Experimental Procedures"), in order to limit aggregation (29) that distorts the calorimetric traces and impairs deconvolution processes. Fig. 5 illustrates the range of stabilities encountered within the DNA ligase family, and Table III provides the thermodynamic parameters associated with thermal unfolding recorded by microcalorimetry. As indicated by the large differences in transition temperature T_{max}, the psychrophilic enzyme is by far the least stable when compared with its mesophilic and thermophillic homologues. In addition, the lowest calorimetric enthalpy, representing the total heat absorbed during unfolding, is recorded for *Ph*lig, underlining its weak thermostability. Deconvolution of the excess heat capacity (C_p) functions revealed one, two, and three subsequent transitions for *Ph*lig, *Ec*lig, and *Ts*lig, respectively (Fig. 5 and Table III), pointing out the presence in the enzymes of an increased number of domains of distinct stability in the order psychrophile → mesophile → thermophile, also corresponding to a decrease of unfolding cooperativity.

The absence of heat absorption effects on rescanning of denatured samples indicates that thermal unfolding of the three enzymes studied is irreversible. The deviation from a two-sate model was further confirmed by the fact that the $\Delta H_{cal}/\Delta H_{eff}$ ratio for the three enzymes exceeds unity (not shown). The irreversible conformational unfolding of DNA ligases is also highlighted by the scan-rate dependence of their apparent T_{max} (Fig. 6*A*), revealing that the thermal denaturation of these proteins is kinetically controlled. Analysis of the thermodynamic parameters of activation for the denaturation process (Fig. 6*B* and Table IV) indicates that, as expected, the denaturation rate is highest for *Ph*lig (higher k_{denat}) and correspondingly, the energy barrier, $\Delta G^{\#}$, is lowest. However, E_a, $\Delta H^{\#}$ and $T\Delta S^{\#}$ are all highest for the psychrophile, indicating that the lower thermostability of the cold-adapted DNA ligase is due to an unfavorable entropic contribution. The complex unfolding pattern of *Ts*lig (Fig. 5) precludes such analysis of the kinetically driven denaturation.

Chemical Stability of DNA Ligases—The stability of the *Ph*lig, *Ec*lig, and *Ts*lig was further investigated by GdmCl-induced unfolding monitored by intrinsic fluorescence. As shown in Fig. 7, these enzymes unfold according to a three-state pathway, involving a stable intermediate between the native and unfolded states. For the three enzymes, unfolding occurs at distinct denaturant concentrations, with a direct relation between the unfolding transition and the above-mentioned thermal stability. Reversibility of unfolding allowed the determination of the thermodynamic parameters (Table V), *i.e.* $\Delta G(H_2O)$ (conformational stability in the absence of denaturant), m (slope of the transition, representing the unfolding cooperativity), and C_m (concentration of GdmCl at the transition midpoint). Compared with *Ec*lig and *Ts*lig, the psychrophilic *Ph*lig exhibits the lowest $\Delta G(H_2O)$ and C_m values, indicating its weak stability. In addition, the cold-adapted enzyme possesses the highest m value, reflecting the highest unfolding cooperativity during chemical unfolding.

DISCUSSION

Protein Structure and Active Site Destabilization—The three-dimensional modeling of the three extremophilic DNA ligases *Ph*lig, *Ec*lig, and *Ts*lig extend previous observations made for the N-terminal domain of *Ph*lig (19) and provide further evidence for the structural determinants implicated in the adaptation to low temperatures of *Ph*lig. Our results suggest that the active site of the cold-enzyme is destabilized by an excess of hydrophobic surfaces and contains a decreased number of charged residues compared with its thermophilic counterpart. These findings are in perfect agreement with the kinetic parameters determined for both enzymes (19). Indeed, k_{cat} is believed to be the most important adaptive parameter for *Ph*lig hence compensating for the effect of low temperatures on the catalytic rate, while for *Ts*lig, the adaptive parameter is expected to be K_m for nicked DNA, which is prone to melting at high temperatures. In the latter, the increase of positively charged amino acids within the active site is likely to facilitate the interaction with the oppositely charged DNA substrate,

TABLE V

Thermodynamic parameters of GdmCl-induced unfolding of Phlig, Eclig and Tslig, as obtained from the analysis of the equilibrium transitions

Parameters are determined from data shown in Fig. 7.

Enzyme[a]	$\Delta G(H_2O)$	$\Sigma\Delta G(H_2O)$	m	Σm	C_m
	kJ mol^{-1}	*kJ mol*$^{-1}$	*kJ mol*$^{-1}$	*kJ mol*$^{-1}$	*M*
*Ph*lig					
$f_N^{N\text{-}I}$	8.4 ± 0.6	27.0	27.7 ± 2.3	43.4	0.3
$f_N^{I\text{-}U}$	18.6 ± 2.9		15.7 ± 2.2		1.2
*Ec*lig					
$f_N^{N\text{-}I}$	12.8 ± 1.2	31.1	15.5 ± 2.0	26.1	0.8
$f_N^{I\text{-}U}$	18.3 ± 3.9		10.6 ± 1.9		1.7
*Ts*lig					
$f_N^{N\text{-}I}$	18.2 ± 3.4	60.4	11.2 ± 1.8	21.4	1.6
$f_N^{I\text{-}U}$	42.2 ± 4		10.2 ± 1.0		4.2

[a] All thermodynamic parameters were determined according to Ref. 26; $C_m = \Delta G(H_2O)/m$.

leading to an improved K_m. Determination of the composition of the accessible surface of the whole molecule also points out an increase of the charged surface in the order psychrophile → mesophile → thermophile. Such increase could lead to an increase of the ion pairs at the surface of *Ts*lig, that could take part to its increased stability. Indeed, ion pairs in solvent-exposed regions of thermophilic enzymes are believed to represent a major key in the adaptation of these enzymes at high temperatures (36, 37). Analysis of the N-terminal domain of *Ph*lig also revealed a significant increase of the degree of exposure of hydrophobic residues to solvent, which is expected to destabilize the protein structure (19). While the model of the entire psychrophilic enzyme confirmed this finding, it was experimentally demonstrated by ANS-binding experiments. Indeed, most native globular proteins do not bind ANS since their hydrophobic core is well protected from the solvent by the rigid packing of side chains (34). However, when native proteins exhibit hydrophobic sites exposed to the solvent, a strong affinity for the dye is observed (34, 35). In the case of *Ph*lig, the strong enhancement of fluorescence intensity of ANS clearly demonstrates the exposure to solvent of hydrophobic clusters. The latter are likely to take part to an entropy-driven destabilization of the cold-adapted enzyme.

Activity at Low Temperatures—Our activity results point out that the cold-adapted *Ph*lig is characterized by a shift of the optimal activity toward low temperatures and an increased specific activity at low and moderate temperatures compared with its mesophilic and thermophilic counterparts. Such increase of activity seems to be due to a higher resilience of the structure, and of the active site. The proposal for a destabilized active site in *Ph*lig is indeed supported by the comparison of the thermodependence of the activity and denaturation of *Ph*lig and *Ec*lig. In the former, the active site is even more heat-labile than the protein structure, since the activity is lost below any significant conformational change. In contrast, the loss of activity of *Ec*lig correlates with that of structural denaturation, showing that structural unfolding is a main determinant for the loss of activity at high temperatures.

Conformational Flexibility—Thermophily is generally correlated with the rigidity of a protein, whereas psychrophily, at the opposite end of the temperature scale, is expected to be characterized by an increase of the plasticity or flexibility of appropriate parts of the molecular structure in order to compensate for the lower thermal energy provided by the low temperature habitat (38, 39). This plasticity would enable a good complementarity with the substrate at a low energy cost, thus explaining the high specific activity of psychrophilic enzymes, but in return would be responsible for the weak thermal stability of these enzymes. The flexibility concept still gives rise to controversy since some reports do not fully support this hypothesis (13–14, 23, 40). However, in such cases, the techniques used suffered from the disadvantage of being a measure of the global flexibility of the proteins over inappropriate time scales, while it is likely that the increased flexibility of cold-adapted enzymes is local and on the microsecond to millisecond timescale, *i.e.* directly related to the active site and catalytic activity. Conformational flexibility of *Ph*lig and its mesophilic and thermophilic homologues was probed by dynamic fluorescence quenching, using acrylamide as quencher. In this technique, the decrease of fluorescence arising from diffusive collisions between the quencher and the fluorophore reflects the ability of the quencher to penetrate accessible regions of the protein (including the active site) and can consequently be viewed as an index of protein permeability (27). In addition, it measures conformational motions over a large timescale (picoseconds to seconds) as it is a dynamic process. Acrylamide quenching experiments performed on the three DNA ligases clearly indicate that *Ph*lig is more flexible than *Ec*lig and *Ts*lig, in a temperature range where the native state prevails. Such flexibility can contribute to the high activity in the low temperature habitat, but also leads to a reduced stability of the molecular edifice.

Conformational Stability—A common characteristic of nearly all psychrophilic enzymes studied so far is their low stability in comparison with their mesophilic homologues. This feature has been demonstrated by the drastic shift of their apparent optimal temperature of activity, the low resistance of the protein to denaturing agents and the high propensity of the structure to unfold at moderate temperatures. The decreased stability of psychrophilic enzymes, in addition to their increased low temperature activity, suggests that there is a direct link between activity and stability *i.e.* maintenance of activity at low temperatures requires the weakening of intramolecular forces which results in reduced stability. The lower stability of psychrophilic enzymes, brought about by a weakening of intramolecular forces contributing to the cohesion of the native protein molecule, may arise either from a general reduction in strength of intramolecular forces (global flexibility), or from weakened interactions in one or a few important regions of the structure (localized flexibility). Investigation of the thermal stability of *Ph*lig by DSC reveals that this enzyme possesses a fragile molecular edifice that is uniformly unstable (one deconvolution unit) and stabilized by fewer weak interactions (decreased ΔH_{cal}) than its mesophilic and thermophilic homologues. It is worth mentioning that *Ph*lig displays the lowest calorimetric enthalpy ΔH_{cal} as well as the lowest T_m ever recorded for cold-adapted enzymes, underlining its strong psychrophilic character through a low conformational stability. Such decreased stability is also highlighted by GdmCl-induced unfolding in which *Ph*lig is characterized by the lowest $\Delta G(H_2O)$ and C_m values.

Further advances in the understanding of the activity/stability relationship can be drawn from the analysis of irreversible thermal unfolding of the cold-adapted DNA ligase and its

mesophilic counterpart. Our results show an increase in free energies of activation $\Delta G^{\#}$ from *Ph*lig to *Ec*lig, reflecting that the same denaturation rate k_{denat} is reached at increasing temperatures (see also Table IV). The small differences in both $\Delta G^{\#}$ values arise however from large differences in the enthalpic and entropic contributions. Indeed, the low $\Delta G^{\#}$ value recorded for *Ph*lig corresponds to the largest $\Delta H^{\#}$ and $T\Delta S^{\#}$ contributions, and conversely for *Ec*lig. Such trend has already been noticed for a few psychrophilic enzymes (17, 18) and thus seems to be a common property of psychrophilic enzymes.

The low kinetic barrier ($\Delta G^{\#}$) recorded for the psychrophilic enzyme allows in fact unfolding at a high rate, leading to a symmetrical and relatively narrow denaturation peak in microcalorimetry (Fig. 5), and consequently to high activation energy *Ea* and high $\Delta H^{\#}$. This reflects a high cooperativity of unfolding for the psychrophilic enzyme, that probably originates from the lower number of interactions required to disrupt the active conformation. The large entropic contribution noticed in *Ph*lig suggests that its transition state is more disordered than that of its mesophilic counterpart, probably due to the fact that at any specific temperature, more interactions are broken into the psychrophile. The entropy loss associated with hydration of nonpolar groups upon denaturation can also contribute significantly to the differences in entropic contribution between *Ph*lig and *Ec*lig. Indeed, in the case of the mesophilic enzyme and more particularly in the thermophilic counterpart, an increased proportion of nonpolar groups are exposed upon unfolding, increasing the order of water molecules and therefore decreasing the entropy change relative to *Ph*lig. All together, our results perfectly fit those obtained for the icefish glutamate dehydrogenase (16), a cold-adapted α-amylase (18) and xylanase (17), demonstrating that thermolability of psychrophilic enzymes is entropically driven. The contradictory result obtained by Siddiqui *et al.* (15) with the elongation factor 2 from a psychrotolerant archae is likely to arise from an unusual broader DSC profile of the cold enzyme (even though associated with a lower T_m) than that of the thermophilic homologue.

Concluding Remarks—Until recently, the activity/flexibility/stability relationship within psychrophilic enzymes was still appreciated with caution. However, the results obtained for the three DNA ligases adapted to different thermal habitats clearly establish a link between activity, flexibility, and stability. The cold-adapted DNA ligase is characterized by a high activity at low temperatures, a high flexibility and a low stability especially at the active site. These results are in perfect agreement with those recently obtained from studies performed on extremophilic α-amylases (18) and xylanases (17). Therefore, the emerging picture suggests that psychrophilic enzymes are characterized by increased catalytic efficiency attributed to an increase of the flexibility of appropriate parts of the molecular structure, in order to compensate for the lower thermal energy provided by the low temperature habitat. In return, this flexibility would be responsible for the weak thermal and chemical stabilities of cold-adapted enzymes.

Acknowledgments—We thank N. Gérardin and R. Marchand for their skilful technical assistance. We also thank F. Biemar, T. Collins, S. D.'Amico, and M. Vanhove for helpful assistance and discussions.

REFERENCES

1. Deming, J. W. (2002) *Curr. Opin. Microbiol.* **5,** 301–309
2. Blochl, E., Rachel, R., Burggraf, S., Hafenbradl, D., Jannasch, H. W., and Stetter, K. O. (1997) *Extremophiles* **1,** 14–21
3. Gerday, C., Aittaleb, M., Arpigny, J. L., Baise, E., Chessa, J. P., Garsoux, G., Petrescu, I., and Feller, G. (1997) *Biochim. Biophys. Acta* **1342,** 119–131
4. Russell, N. J. (1998) *Adv. Biochem. Eng. Biotechnol.* **61,** 1–21
5. Demirjian, D. C., Moris-Varas, F., and Cassidy, C. S. (2001) *Curr. Opin. Chem. Biol.* **5,** 144–151
6. Levy, M., and Miller, S. L. (1998) *Proc. Natl. Acad. Sci. U. S. A.* **95,** 7933–7938
7. Wintrode, P. L., Miyazaki, K., and Arnold, F. H. (2000) *J. Biol. Chem.* **275,** 31635–31640
8. Kumar, S., Tsai, C. J., and Nussinov, R. (2002) *Biochemistry* **41,** 5359–5374
9. Smalas, A. O., Leiros, H. K., Os, V., and Willassen, N. P. (2000) *Biotechnol. Annu. Rev.* **6,** 1–57
10. Cavicchioli, R., Siddiqui, K. S., Andrews, D., and Sowers, K. R. (2002) *Curr. Opin. Biotechnol.* **13,** 253–261
11. D'Amico, S., Claverie, P., Collins, T., Georlette, D., Gratia, E., Hoyoux, A., Meuwis, M. A., Feller, G., and Gerday, C. (2002) *Philos. Trans. R. Soc. Lond. B Biol. Sci.* **357,** 917–925
12. Miyazaki, K., Wintrode, P. L., Grayling, R. A., Rubingh, D. N., and Arnold, F. H. (2000) *J. Mol. Biol.* **297,** 1015–1026
13. Svingor, A., Kardos, J., Hajdu, I., Nemeth, A., and Zavodszky, P. (2001) *J. Biol. Chem.* **276,** 28121–28125
14. Fields, P. A. (2001) *Comp. Biochem. Physiol. A Mol. Integr. Physiol.* **129,** 417–431
15. Siddiqui, K. S., Cavicchioli, R., and Thomas, T. (2002) *Extremophiles* **6,** 143–150
16. Ciardiello, M. A., Camardella, L., Carratore, V., and di Prisco, G. (2000) *Biochim. Biophys. Acta* **1543,** 11–23
17. Collins, T., Meuwis, M. A., Gerday, C., and Feller, G. (2003) *J. Mol. Biol.* **328,** 419–428
18. D'Amico, S., Gerday, C., and Feller, G. (2003) *J. Biol. Chem.* **278,** 7891–7896
19. Georlette, D., Jonsson, Z. O., Van Petegem, F., Chessa, J.-P., Van Beeumen, J., Hubscher, U., and Gerday, C. (2000) *Eur. J. Biochem.* **267,** 3502–3512
20. Sriskanda, V., Schwer, B., Ho, C. K., and Shuman, S. (1999) *Nucleic Acids Res.* **27,** 3953–3963
21. Thorbjarnardóttir, S. H., Jónsson, Z. O., Andresson, O. S., Kristjánsson, J. K., Eggertsson, G., and Pálsdóttir, A. (1995) *Gene* (*Amst.*) **161,** 1–6
22. Lee, J. Y., Chang, C., Song, H. K., Moon, J., Yang, J. K., Kim, H. K., Kwon, S. T., and Suh, S. W. (2000) *EMBO J.* **19,** 1119–1129
23. Hernandez, G., Jenney, F. E., Jr., Adams, M. W., and LeMaster, D. M. (2000) *Proc. Natl. Acad. Sci. U. S. A.* **97,** 3166–3170
24. Timson, D. J., and Wigley, D. B. (1999) *J. Mol. Biol.* **285,** 73–83
25. Pace, C. N. (1986) *Methods Enzymol.* **131,** 266–280
26. Vanhove, M., Guillaume, G., Ledent, P., Richards, J. H., Pain, R. H., and Frere, J. M. (1997) *Biochem. J.* **321,** 413–417
27. Lakowicz, J. (1983) *Principles of Fluorescence Spectroscopy*, pp. 257–301, Plenum Press, New York
28. Feller, G., d'Amico, D., and Gerday, C. (1999) *Biochemistry* **38,** 4613–4619
29. Goldberg, M. E., Expert-Bezançon, N., Vuillard, L., and Rabilloud, T. (1995) *Fold. Des.* **1,** 21–27
30. Matouschek, A., Matthews, J. M., Johnson, C. M., and Fersht, A. R. (1994) *Protein Eng.* **7,** 1089–1095
31. Sanchez-Ruiz, J. M., Lopez-Lacomba, J. L., Cortijo, M., and Mateo, P. L. (1988) *Biochemistry* **27,** 1648–1652
32. Lonhienne, T., Gerday, C., and Feller, G. (2000) *Biochim. Biophys. Acta* **1543,** 1–10
33. Sriskanda, V., and Shuman, S. (2002) *J. Biol. Chem.* **277,** 9695–9700
34. Stryer, L. (1965) *J. Mol. Biol.* **13,** 482–495
35. Semisotnov, G. V., Rodionova, N. A., Razgulyaev, O. I., Uversky, V. N., Gripas, A. F., and Gilmanshin, R. I. (1991) *Biopolymers* **31,** 119–128
36. Kumar, S., and Nussinov, R. (2001) *Proteins* **43,** 433–454
37. Chakravarty, S., and Varadarajan, R. (2002) *Biochemistry* **41,** 8152–8161
38. Hochachka, P. W., and Somero, G. N. (1984) *Biochemical Adaptations*, pp. 355–449, Princeton University Press, Princeton
39. Fields, P. A., and Somero, G. N. (1998) *Proc. Natl. Acad. Sci. U. S. A.* **95,** 11476–11481
40. Fitter, J., and Heberle, J. (2000) *Biophys. J.* **79,** 1629–1936